

1 A high-spatial resolution soil carbon and nitrogen dataset for the
2 northern permafrost region, based on circumpolar land cover
3 upscaling

4

5

6 Juri Palmtag¹, Jaroslav Obu², Peter Kuhry^{3,4}, Andreas Richter⁵, Matthias B. Siewert⁶, Niels Weiss⁷;
7 Sebastian Westermann² and Gustaf Hugelius^{3,4}

8 ¹Department of Human Geography, Stockholm University, Stockholm, Sweden; ²University of Oslo,
9 Department of Geosciences, Sem Sælands vei 1, 0316 Oslo, Norway; ³Department of Physical Geography,
10 Stockholm University, Stockholm, Sweden; ⁴Bolin Centre for Climate Research, Stockholm University,
11 Stockholm, Sweden; ⁵ Centre for Microbiology and Environmental Systems Science, University of Vienna,
12 Vienna; ⁶Department of Ecology and Environmental Science, Umeå University, Umeå, 901 87, Sweden;
13 ⁷Northwest Territories Geological Survey, Government of the Northwest Territories, Yellowknife NT X1A
14 1K3, Canada.

15

16 Corresponding author: Juri Palmtag (juri.palmtag@humangeo.su.se)

17

18

19

20

21

22 **Abstract**

23 Soils in the northern high latitudes are a key component in the global carbon cycle; the northern permafrost region
24 covers 22% of the Northern Hemisphere and holds almost twice as much carbon as the atmosphere. Permafrost soil
25 organic matter stocks represent an enormous long-term carbon sink which is in risk of switching to a net source in the
26 future. Detailed knowledge about the quantity and the mechanisms controlling organic carbon storage is of utmost
27 importance for our understanding of potential impacts of and feedbacks on climate change. Here we present a
28 geospatial dataset of physical and chemical soil properties calculated from 651 soil pedons encompassing more than
29 6500 samples from 16 different study areas across the northern permafrost region. The aim of our dataset is to provide
30 a basis to describe spatial patterns in soil properties, including quantifying carbon and nitrogen stocks, turnover times,
31 and soil texture. There is a particular need for spatially distributed datasets of soil properties, including vertical and
32 horizontal distribution patterns, for modelling at local, regional or global scales. This paper presents this dataset,
33 describes in detail soil sampling, laboratory analysis and derived soil geochemical parameters, calculations and data
34 clustering. Moreover, we use this dataset to estimate soil organic carbon and total nitrogen storage estimates ~~within~~
35 ~~the soil area of~~~~in~~ soils in the northern circumpolar permafrost region ($17.9 \times 10^6 \text{ km}^2$) using the ESA's Climate Change
36 Initiative (CCI) Global Land Cover dataset at 300 m pixel resolution. We estimate organic carbon and total nitrogen
37 stocks on a circumpolar scale (excluding Tibet) for the 0-100 cm and 0-300 cm soil depth to ~~be~~ 380 Pg and 813 Pg
38 for carbon and 21 Pg and 55 Pg for nitrogen, respectively. ~~Of which 48% of the area is within the land-cover class~~
39 ~~forest with a total SOC and TN storage for 0-300 cm of 35% and 36%, respectively.~~ Our organic carbon estimates
40 agree with previous studies, with most recent estimates of 1000 Pg (– 170 to +186 Pg) to 300 cm depth ~~but show~~
41 ~~different spatial patterns.~~ Two separate datasets are freely available on the Bolin Centre Database repository, [Dataset](#)
42 [references and DOIs are presented in the “Data access” section in the end.](#) [\(<https://doi.org/10.17043/palmtag-2022-pedon-1>](https://doi.org/10.17043/palmtag-2022-pedon-1) [Palmtag et al., 2022a](#) and [\(<https://doi.org/10.17043/palmtag-2022-spatial-1>](https://doi.org/10.17043/palmtag-2022-spatial-1) [Palmtag et al., 2002b](#)).

Formatted: English (United States)

45 **1. Introduction**

46 Permafrost soils represent a large part of the terrestrial carbon reservoir and form a significant and climate-sensitive
47 component of the global carbon cycle (Hugelius et al., 2014). High-latitude ecosystems are experiencing rapid climate
48 change causing warming of ~~the soil temperatures~~, thawing of permafrost, and fluvial and coastal erosion (Biskaborn
49 et al., 2019; Fritz et al., 2017). Warming enhances the decomposition of organic matter (OM) by microorganisms,
50 which in turn produces carbon dioxide, methane, and nitrous oxide. The release of these greenhouse gases to the
51 atmosphere ~~would in turn generate further climate change, resulting in is accelerating and could potentially constitute~~
52 a positive feedback on global warming (Turetsky et al., 2020). To better predict the magnitude and effect of
53 environmental changes in the permafrost region, improved data on the properties and quantities of carbon and nitrogen
54 stored in these climate vulnerable soils are needed.

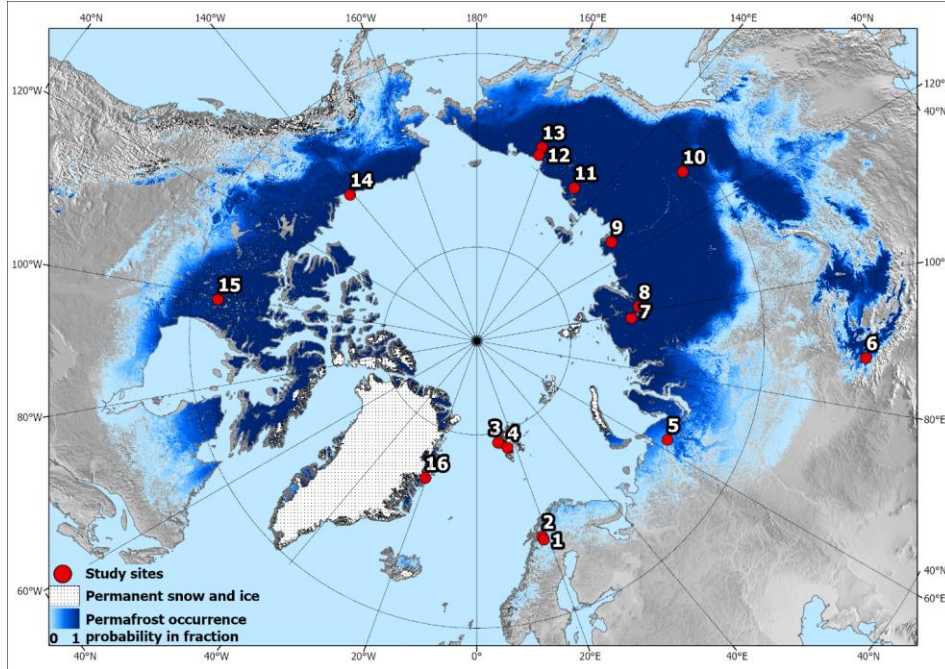
Formatted: English (United States)

55 In many cases, a lack of observational data for parameterization or evaluation can limit model development or accurate
56 model projections (Flato, 2011). Soil properties such as **organic matter** (OM) content, soil texture and soil moisture or
57 their derivatives are commonly used to parametrize, train or validate models (e.g. Oleson et al., 2010). Yet, the
58 representation of northern soil profiles in global datasets remains limited (Köchy et al., 2015; Batjes, 2016), the
59 northern circumpolar permafrost region ($20.6 \times 10^6 \text{ km}^2$) in which permafrost can occur accounts for 22% of the
60 Northern Hemisphere exposed land area (Obu et al, 2019).

61 Many previous studies have shown a robust relationship between land cover and soil organic carbon (SOC)
62 distribution, making land cover datasets useful for upscaling **estimates** from soil profiles to full landscape coverage
63 (e.g. Kuhry et al., 2002; Hugelius, 2012; Palmtag et al., 2015; Siewert et al., 2015; Wojcik et al., 2019). Here we
64 describe the compilation of a harmonized soil dataset for permafrost-affected landscapes derived from 15 different
65 high latitude sites and one high alpine study site in Canada, Greenland, Svalbard, Sweden, and Russia (Fig. 1; Table
66 1). In total, 651 soil pedons contain information from up to 6529 samples on carbon and nitrogen content, carbon to
67 nitrogen (C/N) ratio, isotopic composition, texture (sand, silt+clay) and coarse fraction content, land cover type, wet
68 and dry bulk density, calculated volumetric contents for ice/water, and volumetric content of organic soil material,
69 mineral soil material and air. In addition, soil pedon descriptions include metadata on actual sampling site, coordinates
70 and elevation, slope and aspect, drainage, **cover percentage of** stones and boulders, landform, and maximum sampling
71 depth. Site data **was were** upscaled to the northern circumpolar permafrost region using the European Space Agency
72 (ESA) Climate Change Initiative (CCI) Global Land Cover dataset at 300 m pixel resolution, which is the very first
73 long-term global land cover time series product.

74 This study has two main **objectivesaims**. Firstly, the core objective of this dataset is to provide a harmonized, high
75 resolution, quality controlled, and contextualized soil pedon dataset with a focus on SOC, nitrogen and other
76 parameters essential to determine the role of northern permafrost region soils in the climate system. Secondly, to use
77 the dataset and an existing spatial product for upscaling to provide a new and independent estimate of the soil organic
78 carbon and total nitrogen (TN) storage estimates within the northern circumpolar permafrost region. **The data set aims**
79 **to provide the scientific community with new and improved geospatial products quantifying carbon and nitrogen pools**
80 **within the northern circumpolar permafrost region**. Particularly, the extensive metadata on soil properties included for
81 many samples when available (texture, volumetric densities, active layer depth, ice content, isotopic composition, etc.)
82 are of great importance and can be used to identify and model the processes responsible for the current and future
83 carbon balance.

84



85

86 Figure 1: Overview map with location of the 16 sampling sites (see Table 1). Blue shading indicates permafrost
 87 probability (dark hues showing higher permafrost occurrence probability), based on an equilibrium state model for
 88 the temperature at the top of the permafrost (TTOP) for the 2000–2016 period (Obu et al., 2019). North Pole Lambert
 89 azimuthal equal area projection (datum: WGS 84). Base map: Made with Natural Earth.

90

91 **2. Methods**

92 **2.1 Dataset structure**

93 The dataset contains 6529 analyzed samples from 651 soil pedons in 16 different sampling locations across the
 94 northern permafrost region (Fig 1; Table 1) (Palmtag et al., 2022a, b). Each sampled pedon was described and
 95 classified according to land cover type. Land cover is defined as the biophysical cover of the Earth's terrestrial surface
 96 such as different vegetation types, water, and bare ground.

97

98 Table 1: Summary of all study sites

Nr.	Study area	Country	Long	Lat	n=pedons	Reference
1	Tarfala	Sweden	18.63° E	67.91° N	55	Fuchs et al., 2015
2	Abisko	Sweden	18.05° E	68.33° N	125	Siewert, 2018
3	Ny Ålesund	Norway	11.83° E	78.93° N	28	Wojcik et al., 2019
4	Adventdalen	Norway	16.04° E	78.17° N	48	Weiss et al., 2017
5	Seida, Usa River Basin	Russia	62.55° E	67.35° N	44	Hugelius et al., 2009; 2011
6	Aktru, Altai mountains	Russia	87.47° E	50.05° N	39	Pascual et al., 2020
7	Logata, Taymyr	Russia	98.42° E	73.43° N	31	Palmtag et al., 2016
8	Arymas, Taymyr	Russia	101.90° E	72.47° N	35	Palmtag et al., 2016
9	Lena Delta	Russia	126.22° E	72.28° N	56	Siewert et al., 2016
10	Spasskaya Pad	Russia	129.46° E	62.25° N	33	Siewert et al., 2015
11	Tjokurdach	Russia	147.48° E	70.83° N	27	Siewert et al., 2015; Weiss et al., 2016
12	Shalaurovo	Russia	161.55° E	69.32° N	22	Palmtag et al., 2015
13	Cherskiy	Russia	161.30° E	68.45° N	15	Palmtag et al., 2015
14	Herschel Island	Canada	-139.09° W	69.58° N	42	Siewert et al., 2021
15	Tulemalu Lake	Canada	-99.16° W	62.55° N	16	Hugelius et al., 2010
16	Zackenberg	Greenland	-20.50° W	74.45° N	35	Palmtag et al., 2015; 2018

99

100

101 Land cover products are commonly satellite derived and sometimes globally available. We opted for a two-tier
 102 approach, where more classes can be used in products with higher thematic or spatial resolution (Table 2). First, we
 103 differentiated land cover into 75 primary tier classes (Tier I) which represent the major land cover types: Forest, forest,
 104 Tundra, Tundratundra, Wetland, wetland, Water, Barren, barren, Permanent Snow/ice and Yedoma. Although Yedoma is a
 105 sedimentary deposit and not a typical land cover class, it was added due to its large areal extent, special soil organic
 106 matter (SOM) and ground ice properties, as well as soil characteristics (Strauss et al., 2017; Weiss et al., 2016).
 107 Subsequently, Tier I classes were subdivided into 140 Tier II subclasses (Table 2). The two-class tier structure provides
 108 more detailed information for each specific land cover class. Depending on the accuracy of the land cover data
 109 available for specific sampling sites, the best fitting Tier level can be used.

110

111

112 Table 2: Hierarchical structure of the two-tier land cover class system applied to the pedons based on field
113 observations.

TIER I		TIER II
1	Forest	1.1 Deciduous broadleaf forest 1.2 Evergreen needleleaf forest 1.3 Deciduous needleleaf forest
2	Tundra	2.1 Shrub tundra 2.2 Graminoid / forb tundra
3	Wetland	3.1 Permafrost wetlands 3.2 Non-permafrost wetlands
4	Water bodies	4.1 Lakes 4.2 Streams
5	Barren	5.1 Barren
6	Snow/Ice	6.1 Snow/Ice
7	Yedoma	7.1 Yedoma tundra 7.2 Yedoma forest

114 2.1.1 Class definitions of soil pedons to land cover types

115 All sampling sites were classified with Tier I descriptions using field descriptions and, where possible, assigned a
 116 more detailed (Tier II) description. All pedons were assigned to land cover classes based on field observations and
 117 photographs. The forest class was used for sparse to dense forests, further separated into three different Tier II classes:
 118 deciduous broadleaf, evergreen needleleaf and deciduous needleleaf forest. Tundra is separated in Tier II to shrub
 119 tundra (dominated by erect shrubs >50cm height) and graminoid / forb tundra (with low growth heath vegetation or
 120 graminoid dominated). Wetland includes terrain that is saturated with water for sufficient time of the year to promote
 121 aquatic soil processes with low oxygen conditions and occurrence of vegetation fully adapted to these conditions, as
 122 well as all types of peatlands. We applied a classification that is adapted from the Canadian system. The following
 123 (National Wetlands Working Group, 1997) describing the wetlands in the field and following types of wetlands
 124 described in the field were included to the Tier I wetland class: organic wetland, mineral, seasonal, permanent,
 125 ombrotrophic and minerotrophic wetlands. The permafrost status within the top 2 m of a site was
 126 used to distinguish in Tier II the permafrost wetlands and the non-permafrost wetlands. Tier II wetland classes are
 127 wetlands with permafrost within the upper 2 m from the soil surface and wetlands without permafrost within the upper

128 **2 m from the soil surface.** Although a substantial part of the northern circumpolar permafrost region is classified as
129 water ($0.98 \times 10^6 \text{ km}^2$) or permanent snow/ice ($0.06 \times 10^6 \text{ km}^2$), no soil sample or pedon data from these classes are
130 included in the database. **The** ~~For the same reason the~~ Tibetan permafrost region was ~~also excluded from not included~~
131 ~~in our estimates as none of the sampling sites originated from that area.~~ The class barren includes land cover types
132 such as exposed bedrock, boulder fields, talus slopes, debris cones, rock glaciers, where soil is either completely
133 absent, or occurs only in minor patches (<10 % area) or in between boulders. The land cover class Yedoma is defined
134 as areas ~~in Siberia, Alaska, and Yukon~~ underlain by late Pleistocene ice-rich syngenetic permafrost deposits. **We used**
135 ~~the spatial extent for the Yedoma domain from Strauss et al. (2017) which occupied an area of 570,000 km² from here~~
136 ~~ESA CCI land cover product, which occupy an area of about 1,000,000 km² in Siberia, Alaska, and Yukon (Strauss~~
137 ~~et al., 2017)~~. Tier II divides the Yedoma domain into Yedoma tundra and Yedoma forest.

138 **2.2 Soil sampling and soil analyses**

139 **The main aim of the field studies compiled in the current dataset was to perform SOC/TN pool inventories of each**
140 **study area considering different land cover types, geomorphological landforms and soil properties.** Field soil sampling
141 took place in summer months (late June to early September) between 2006 and 2019, most frequently in August or
142 September in order to capture the maximum seasonal thaw (active layer) depth at each site. **Active layer thickness was**
143 **measured at each location using a graduated steel probe or measuring tape in excavated soil pits.** **At most sites, a**
144 **A** stratified sampling scheme **(582 out of 651)** consisting of linear transects with predefined equidistant intervals of
145 typically 100 to 200 m across all major landscape elements was used, **with on average 37 sampling sites per study**
146 **area.** To ensure that this sampling scheme covered all representative landscape units and types, maps (including
147 vegetation, surficial geology) and remote sensing products (including air photos, satellite imagery, and elevation
148 models) were assessed prior to fieldwork. Detailed field reconnaissance involving visual observation of the
149 manageable study area were conducted before establishing transects. Sampling sites were located and marked at the
150 exact position based on distance to the first sampling point and compass bearing using a hand-held GPS device. This
151 ensured an unbiased location of individual sampling sites. **For some locations, when** ~~w~~hen sufficient time was available
152 in the field, **additional sampling using** a random or stratified random distribution of sampling points was used.
153 Following the field sampling protocol (Figure S1), a site description, soil and in several cases phytomass sampling
154 were conducted at each sampling point.

155 For each pedon, the **top-organic layer (OL) was sampled in three replicates, and** the active layer was sampled from an
156 open soil pit **excavated to the bottom of the active layer, to the bedrock or to at least reach a depth beyond ± 50 cm**
157 **(Fig. 2).** **Deeper unfrozen soil layers were sampled using a steel pipe** (see permafrost sampling below). **The organic**
158 **layer sample was cut out as a block using a pair of scissors or a knife (removing living vegetation), and the block**
159 **volume was measured in the field. The** ~~a~~nd **deeper sections normally using a steel pipe for soil coring in permafrost.**
160 **When possible, samples were also collected from exposures along lake shores or river valleys (Fig. 2).** **Accurate**
161 **determination of soil bulk density (BD) is crucial when converting sample weight to volume or area and is essential**
162 **to calculate SOC stocks. Therefore, special attention was paid to accurate soil volume estimation during field**

163 sampling. The target depth for soil cores was 100 cm, or until bedrock or massive ground ice (e.g. ice-wedges) was
164 reached. Pedons were occasionally extended beyond 100 cm depth, in particular to assess full peat depth and
165 organic/mineral transition in organic soils.

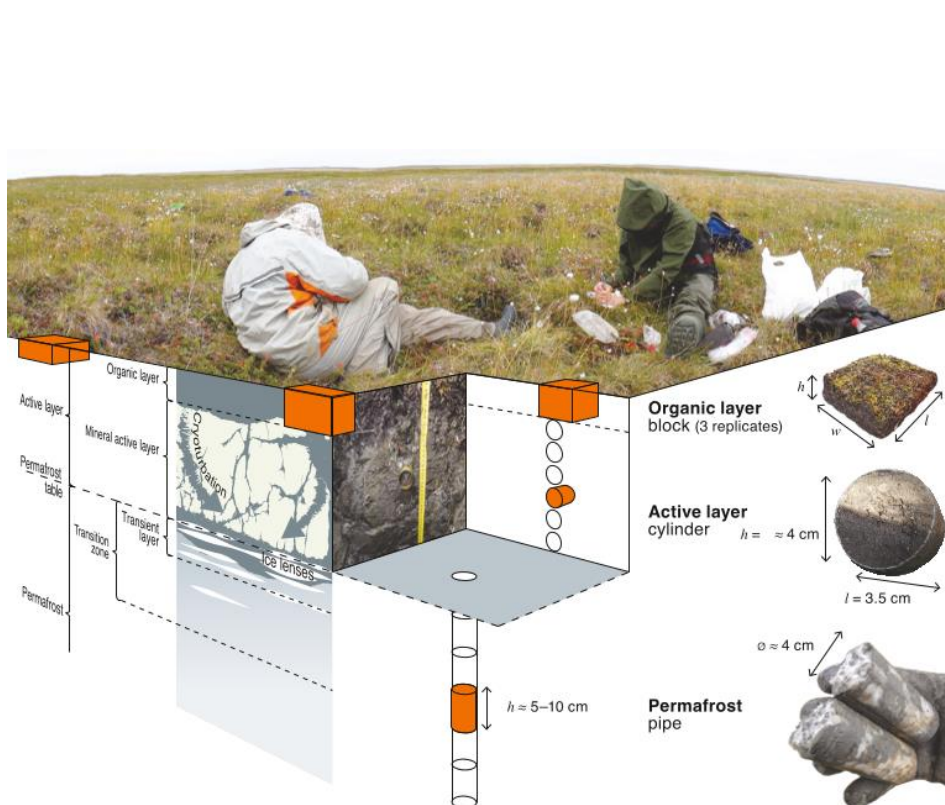
166 The top organic layer samples were cut out as a block using a pair of scissors or a knife (removing living vegetation),
167 measuring the block volume in the field (Fig. 2). Variation in the top organic layer thickness can be substantial and
168 for this reason from most pedons two randomly selected replicates (OL2 & OL3) in addition to the main soil pit were
169 collected (not in peatlands). Active layer samples were collected from a soil pit excavated to the bottom of the active
170 layer, to the bedrock or to reach a depth of ± 50 cm, or in a few cases from natural exposures using 100 cm³ soil
171 sampling rings inserted horizontally into the soil profile. Sampling of the active layer was performed in fixed depth
172 intervals (5–10 cm) or along soil horizon boundaries. During some field campaigns, emphasis was also given to the
173 spatial distribution of soil horizons in the soil pit using perspective corrected photographs to calculate the respective
174 area covered by each horizon, which was then translated into depth increments (Siewert et al. 2016; 2021). For non-
175 permafrost-free wetland sites a Russian peat corer with a 50 cm long chamber was used. After extraction, the core was
176 described and subdivided into smaller increments (generally 5 cm). This resulted typically in about 5–15 samples per
177 sampling site depending on the reached depth.

178 The permafrost section of the soil profile and very deep unfrozen soil layers were sampled using a steel pipe that was
179 hammered into the frozen ground in short (5 to 10 cm) depth increments. The pipe was pulled out after each sampled
180 increment using large pipe wrenches, and the sample was pushed out of the pipe using a steel rod. At several locations
181 permafrost samples were also collected from exposures along lake shores or river valleys where the steel pipe was
182 hammered in horizontally. These steel pipes are industry standardized with an outer diameter of 42.2 mm (1.25 inches),
183 affordable and widely available even in remote locations. A custom made protective hard steel cap placed over the
184 steel pipe greatly extends the usability of the pipe and this method in general. Over time, pipe ends deform from
185 hammer impacts and hard objects such as rocks, and damaged ends can be cut off in the field using a hacksaw. An
186 experienced team of 2–3 persons can sample 4–6 soil pedons in one day using this method. At several locations, soil
187 cores were collected using a handheld motorized rotational Earth Auger (Stihl BT 121) with a 50 cm core barrel and
188 52 mm outside diameter. Following recovery, samples were split lengthwise into two halves: one half was in
189 preparation for analysis. Usually, half of each core was kept as a frozen archive to be used in the event of laboratory
190 error. The remaining half core was analyzed to determine sediment characteristics, volumetric ice content, and
191 gravimetric water content. Disturbance material was removed from the core surface by repeated scraping with a razor
192 blade. All half-cores were then photographed and described in detail. The other half of each core was kept as a frozen
193 archive to be used in the event of laboratory error. Since the

194 When possible, samples were also collected from exposures along lake shores or river valleys (Fig. 2). Accurate
195 determination of soil bulk density (BD) is crucial when converting sample weight to volume or area and is essential
196 to calculate SOC stocks. Therefore, special attention was paid to accurate soil volume estimation during field
197 sampling. The target depth for soil cores was 100 cm, or until bedrock or massive ground ice (e.g. ice-wedges) was

198 reached. Pedons were occasionally often extended beyond 100 cm depth (n = 313), in particular to assess full peat
199 depth and organic/mineral transition in organic soils.

200 All samples were described in the field and packed into sampling bags. Wet or frozen samples were placed in double
201 bags to assure no soil water was lost in transport. For each sampled soil profile, pictures and notes were taken to
202 describe land cover type, landform, elevation, slope and aspect, surface moisture, and surface features. Specific
203 observations regarding the collected sample depths, such as excess ground ice (visual estimate, %), occurrence of
204 large stones (visual estimate, %), colour (general description or using a Munsell scale), soil structure, including signs
205 of cryoturbation, roots and rooting depth were noted. Samples with cryoturbated soil material were marked or rated
206 on a scale from 1 to 3 according to the relative amount of cryoturbated soil material. Soil texture, which refers to
207 particle size and relative content of mineral components (sand, silt+clay) is of importance as it affects the physical
208 and chemical properties of a soil, including cryoturbation (Palmtag and Kuhry, 2018). Soil texture was estimated for
209 most samples using manipulation tests and assessment by hand in the field under varying weather conditions. In case
210 of permafrost samples, subsamples were thawed, analyzed and returned back to the sample bag. ThereforeTo avoid
211 misinterpretation, we decided to combine silt and clay to avoid misinterpretation and refer to them as one fine-grained
212 soil texture class. ~~For a subset of samples, particle size analysis was performed using a Malvern Mastersizer 3000~~
213 ~~laser particle size analyzer (Malvern Instruments Ltd, Malvern, UK), which can analyze particles in the range of 0.01–~~
214 ~~3500 µm in diameter. It measures the intensity of light scattered as a laser beam passes through a dispersed particulate~~
215 ~~sample. A detailed description of these samples is given in Palmtag et al. (2018). For some studies soils were classified~~
216 ~~following the US Soil Taxonomy system (Soil Survey Staff, 2014). The availability of these parameters is consistent~~
217 ~~for most pedons, but the degree of metadata completeness depends on the scope of the original study.~~ The land cover
218 and vegetation community was described at all sites. For many sites, vegetation cover was described in terms of
219 relative plant functional type coverage per square meter. Beyond assigning the profiles to land cover, vegetation data
220 is not included in this database and not further discussed.



221

222 Figure 2: A three-dimensional field sampling protocol with typical soil layers in permafrost ground (reprinted from
 223 Weiss 2017, p.12). The orange shapes represent the different sampling techniques for organic surface layer (block),
 224 active layer sample from an excavated pit (fixed volume cylinder) and permafrost sampling (steel pipe).

225 **2.3 Laboratory analysis**

226 In the laboratory, soil samples ($n=5315$) were weighed before and after oven-drying at $60-70^{\circ}\text{C}$ for at least 24 h (or
 227 until no further weight change was observed) to determine field-moist mass (m_w) and the oven-dried mass (m_d), thus
 228 permitting the calculation of wet bulk density (BD_w) and dry bulk density (BD , g cm^{-3}) using the known sample
 229 volume. In From most cases organic rich and fine grained samples ($n = 3684$), subsamples of around 10 g were dried
 230 again at 105°C to verify dry weight and correct in case not all water was lost at the lower temperature. Remaining
 231 samples which were not dried again, were sand or coarse grain samples and showed in tests no noteworthy differences.
 232 The reason for the main sample being dried at lower temperature is to ensure that samples can be dried in the original
 233 plastic sample bags (without loss of sampled materials) and subsequently used for additional analyses that may be
 234 sensitive to the higher drying temperature (results from such additional analyses are not included here). After drying,
 235 samples were homogenized and sieved to determine the concentration of coarse mineral fragments ($\text{CF}_{>2 \text{ mm}}$, %).
 236 For a subset of samples, particle size analysis was performed using a Malvern Mastersizer 3000 laser particle size

237 analyzer (Malvern Instruments Ltd, Malvern, UK), which can analyze particles in the range of 0.01–3500 μm in
238 diameter. It measures the intensity of light scattered as a laser beam passes through a dispersed particulate sample. A
239 detailed description of these samples is given in Palmtag et al. (2018). Out of 5331 samples where OC % data is
240 available, ~~ss~~subsamples from 4471 samples were burned for 5h at 550°C to obtain organic matter content through
241 loss on ignition (LOI; Heiri et al., 2001), and about ~~half of the~~ every second samples ($n=2960$), ~~was~~ were burned at
242 950°C for 2 h to determine carbonate content (for details, see Palmtag et al., 2015; 2016). To determine the elemental
243 content of carbon and nitrogen (TOC and TN) and their isotopic composition, 2674 samples were analysed using an
244 Elemental Analyser (EA). If LOI~~950~~ following Heiri et al. (2001) indicated presence of inorganic carbon ~~with > 1%~~,
245 samples were acid treated (Abisko, Sweden; Ny Ålesund, Norway; Aktru, Altai mountains, Russia) with hydrochloric
246 acid prior to determination of TOC. To estimate the organic carbon % (OC %) for samples where only LOI was
247 available (44 %), a polynomial regression model ($R^2 = 95\%$) was performed between LOI550 and OC %~~OC~~ from EA
248 on samples for which both analyses were available ~~at study area level~~. In most cases a third or fourth order polynomial
249 regression model was used and applied at study area level.

250 Carbon to nitrogen (~~weight~~) ratios are often used as an indicator for SOM decomposition. As during the metabolic
251 activity by microorganisms more carbon than nitrogen is released, the C/N ratio decreases with a higher degree of
252 humification. This is why C/N ratios usually decrease with depth, as deeper layers are typically older and ~~underwent~~
253 ~~more~~ decomposed ~~over longer periods of time~~ (Kuhry and Vitt, 1996). The C/N ratios ~~T~~ogether with stable
254 carbon isotopes ($\delta^{13}\text{C}$) ~~this~~ can be used to gain insight into the biochemical processes of SOM, botanical origin with
255 depth and the degradation state (Kracht and Gleixner, 2000).

Formatted: Superscript

256 2.4 SOC/TN stock calculations and upscaling soil profile extrapolations

257 Dry and wet bulk density (g cm^{-3}), sample volume (cm^3) and % carbon was used to calculate the volumetric contents
258 of water, organic soil material, mineral soil material and air for each sample. The soil organic carbon content (kg C
259 m^{-2}) was calculated for each sample separately based on dry bulk density (BD, g cm^{-3}), percentage organic C in the
260 sample (OC %~~OC~~), sample thickness T (cm), and coarse fraction correction (CF) (Equation 1). Equation 1 was also
261 used to calculate the TN content, in which OC %~~OC~~ was replaced with %N %.

$$262 \text{SOC}(\text{g C cm}^{-2}) = \text{BD} * \% \text{OC} * (1 - \text{CF}) * T \quad 1$$

263 SOC content for each pedon was calculated by summing up individual samples ~~on 1 cm resolution until the maximum~~
264 ~~sampling depth was reached. The pedons were assigned~~ to a specific ~~land cover class and the SOC content averaged~~
265 ~~for different depth intervals (0–30 cm, 30–50 cm, 50–100 cm, 100–200 cm, 200–300 cm, and summed to 0–100 cm~~
266 ~~and 0–300 cm) until the maximum sampling depth was reached~~. In areas with large stones in the soil column (e.g.
267 alpine areas) or areas with massive ice bodies (e.g. Yedoma deposits), it is also important to deduct the volume of
268 stones or massive ice from the calculations. These additional variables are not included in equation 1, but were
269 accounted for in the SOC calculations at the pedon level. If bedrock was encountered at any point, a SOC content of
270 0 kg C m^{-2} was assigned for the remaining part down to 300 cm depth at that specific sampling site. ~~For calculations,~~

271 the top organic layer calculation is based on the first OL1 sample only. In pedons where some increments were missing
272 or the full sampling depth was not reached, the nearest samples from the same pedon for BD and OC % were
273 interpolated or extrapolated. To avoid overestimation of the SOC storage, such extrapolations were only used where
274 field notes showed that the deposits were homogeneous and bedrock was not reached.

275 Masses of soil components (water (m_w , g), organic matter (m_{OM} , g) and mineral component (m_{min} , g)) were calculated
276 based on the from laboratory results analysis for all the individual samples. The mass of water was calculated as a
277 difference between field-moist mass and oven-dried mass. Organic matter mass was calculated from the OC %
278 and dry sample weight and multiplied by 2, which is a standard conversion factor between SOC and SOM (Pribyl,
279 2010). The mass of the mineral fraction was calculated as a difference between dry sample mass and organic matter
280 mass.

281 Volumetric fractions of soil components were calculated by dividing the volume of the component with the total
282 sample volume (V). We calculated component volumes from mass by assuming the following densities: 1 g/cm³ for water,
283 0.91 g/cm³ for ice, 1.3 g/cm³ for organic matter (Farouki, 1981) and 2.65 g/cm³ mineral
284 component. The volumetric fraction of air was calculated as one minus the sum of the other fractions.

285 2.5 Pedon grouping and SOC/TN upscaling

286 All profiles were assigned to land cover class based on field descriptions. Dry bulk density, SOC density, TN density
287 and the volumetric contents of mineral and organic matter and water and air were averaged according to land cover
288 classes for depths until 3 m using Python scripting language and pandas library (McKinney, 2011). Soil parameters
289 were assigned to pedon sample depth ranges and these were grouped according to land cover classes yielding means
290 and standard deviations for each centimetre of depth. Fractions of soil texture classes (sand and silt + clay) were
291 created using the same procedure by counting occurrences of texture classes within pedons. The values were averaged
292 with 1 cm resolution for the top 10 cm, to 5 cm between 10 and 30 cm and to 10 cm averaged values for below 30 cm
293 of soil depth. Typical soil stratigraphies were generated for each class which can be used as input for permafrost
294 modelling and mapping (e.g. Westermann et al., 2013; 2017; Czekirda et al., 2019).

295 For the upscaling, we used the land cover map from the Global ESA Land cover Climate Change Initiative (CCI)
296 project at 300 m spatial resolution (<http://maps.elie.ucl.ac.be/CCI/viewer/index.php>). The overall classification
297 accuracy, based on 3167 random sampling cases, is stated as 73% (Defourny et al., 2008). The land cover class dataset
298 for upscaling was generated from ESA CCI land cover yearly products from period 2006 to 2015 (corresponding to
299 the sampling period) using majority statistics to define by identifying prevailing land cover classes within this period.
300 The extent of the Yedoma land cover classes was defined from shapefiles of the Yedoma database by Strauss et al.,
301 (2017), where all the layers were used except for QG2500k, which is showing the lowest probability of Yedoma
302 occurrence. While the extent of Yedoma is based on maps of Quaternary deposits, no such maps were used to support
303 upscaling of other soil properties.

304 Since the ESA land cover product uses a different nomenclature for land cover types with different sub-categories,
305 similar classes were amalgamated to fit our tiered land cover system (Table 2). Several minor classes consisting of
306 single pixels spread over the map were generalized and merged with the class surrounding the pixel. The Tier classes
307 “water bodies” and “Snow / ice” occupy substantial areas but were excluded from the SOC storage estimates; this
308 study focuses on terrestrial SOC and TN storage. We defined tier II Yedoma classes (Yedoma tundra and Yedoma
309 forest) according to the ESA CCI Land cover classes coinciding with Yedoma deposits (Table 3).

310 The spatial land cover extent was constrained to the Northern Hemisphere permafrost region indicating probability of
311 permafrost occurrence but not the actual area underlain by permafrost (indicated by permafrost area) (Obu, 2021).
312 This used permafrost region dataset stretches over $17.9 \times 10^6 \text{ km}^2$ of the Northern Hemisphere, and is based on
313 equilibrium state model for the temperature at the top of the permafrost (TTOP) for the 2000–2016 period (Obu et al.,
314 2019).

315 Since the ESA land cover product uses a different nomenclature for land cover types with different sub-categories,
316 similar classes were amalgamated to fit our tiered land cover system (Table 2). Several minor classes consisting of
317 single pixels spread over the map were generalized and merged with the class surrounding the pixel. The Tier classes
318 “water bodies” and “Snow / ice” occupy substantial areas but were excluded from the SOC storage estimates; this
319 study focuses on terrestrial SOC and TN storage. We defined tier II Yedoma classes (Yedoma tundra and Yedoma
320 forest) according to the ESA CCI Land cover classes coinciding with Yedoma deposits (Table 3).

321

322 Table 3: Amalgamation of ESA’s CCI land cover classes with the Tier class system above the Yedoma deposits.

CCI class	ESA CCI landcover	TIER I class	TIER II class
40	Mosaic natural vegetation (tree, shrub, herbaceous cover) (>50 %)	1	1.1 & 57 .2
50	Tree cover, broadleaved, evergreen, closed to open (>15 %)	1	1.1 & 57 .2
60	Tree cover, broadleaved, deciduous, closed to open (>15 %)	1	1.1 & 57 .2
61	Tree cover, broadleaved, deciduous, closed (>40 %)	1	1.1 & 57 .2
70	Tree cover, needleleaved, evergreen, closed to open (>15 %)	1	1.2 & 57 .2
71	Tree cover, needleleaved, evergreen, closed (>40 %)	1	1.2 & 57 .2
72	Tree cover, needleleaved, evergreen, open (15-40 %)	1	1.2 & 57 .2
80	Tree cover, needleleaved, deciduous, closed to open (>15 %)	1	1.3 & 57 .2
90	Tree cover, mixed leaf type (broadleaved and needleleaved)	1	1.1 & 57 .2
100	Mosaic tree and shrub (>50 %) / herbaceous cover (<50 %)	1	1.1 & 57 .2
110	Mosaic herbaceous cover (>50 %) / tree and shrub (<50 %)	1	1.3 & 57 .2
120	Shrubland	2	2.1 & 57 .1
121	Evergreen shrubland	2	2.1 & 57 .1
122	Deciduous shrubland	2	2.1 & 57 .1
130	Grassland	2	2.2 & 57 .1
140	Lichens and mosses	2	2.2 & 57 .1
150	Sparse vegetation (tree, shrub, herbaceous cover) (<15 %)	2	2.1 & 57 .1

152	Sparse shrub (<15 %)	2	2.1 & <u>57.1</u>
160	Tree cover, flooded, fresh or brackish water	3	3.1
180	Shrub or herbaceous cover, flooded, fresh/saline/brackish water	3	3.1
200	Bare areas	5	<u>45.1</u>
201	Consolidated bare areas	5	<u>45.1</u>
202	Unconsolidated bare areas	5	<u>45.1</u>
<u>210</u>	<u>Water bodies</u>	<u>4</u>	<u>4.1</u>
<u>220</u>	<u>Permanent snow and ice</u>	<u>6</u>	<u>6.1</u>

323

324 The upscaling to estimate the total carbon storage in the northern circumpolar permafrost region was performed in
 325 ArcGIS Pro (ESRI, Redlands, CA, USA) by multiplying the mean SOC storage for each tier 1 and tier 2 class with
 326 the spatial extent of the corresponding CCI land cover class. To determine reasonable error estimates for carbon stocks
 327 within the permafrost region, we used a spatially weighed 95 % confidence interval (CI) as described by Thompson
 328 (1992) assuming that our residuals are normally distributed (Hugelius, 2012).

$$329 CI = t * \sqrt{\sum((a_i^2 * SD_i^2)/n_i)} \quad 2$$

330 The CI accounts for the relative spatial extent, carbon stock variations in pedons and number of replicates in each
 331 upscaling class. Replicates were only considered for pedons reaching the full depth, resulting in fewer replicates with
 332 increasing sampling depth. In equation 2: t is the upper $\alpha/2$ of a normal distribution ($t \approx 1.96$), a the % of the area; SD
 333 is the standard deviation, n is to the number of replicates and i refers the specific Tier class.

$$334 CI = t * \sqrt{\sum((a_i^2 * SD_i^2)/n_i)} \quad 2$$

335 **3. Results**

336 **3.1 SOC estimates**

337 Using our pedon based dataset, we obtain SOC stock estimates within the northern circumpolar permafrost region of
 338 379.7 and 812.6 Pg for 0–100 cm and 0–300 cm depth, respectively. Table 4 shows mean SOC storage (kg C m^{-2}
 339 kg C m^{-2}) and total SOC stock for all depth increments, including 95 % confidence intervals. The upscaling using this
 340 new pedon data shows that almost half of SOC in the northern circumpolar permafrost region is stored in the top
 341 meter. The three most abundant classes together (deciduous needleleaf forest, shrub tundra and graminoid / forb
 342 tundra) occupy 67 % of the permafrost region (Table 5) and store the bulkmost of terrestrial SOC in the northern
 343 circumpolar region (74 %). The permafrost wetland class has the largest SOC content to 300 cm with 112.2 kg C m^{-2}
 344 kg C m^{-2} , but has only a small areal coverage in the ESA LCC product (1.4 %) which results in a total SOC storage
 345 contribution of 3.5 % within the permafrost region. Figure 3 illustrates the spatial distribution of total SOC storage
 346 (kg C m^{-2}) to a depth of 0–100 cm and 0–300 cm for the circumpolar permafrost region. Spatially, the SOC distribution

347 is following same pattern and is highlighting mostly permafrost peatlands in Western Siberia, Russia and the Nunavut
348 territory in Canada. Despite that, more than 77% of the area has a SOC storage to a depth of 300 cm below 50 kg m^{-2}
349

350 Table 4: Landscape mean and total SOC storage with 95 % CI for the different depth increments for the northern
351 circumpolar permafrost region, excluding water bodies and permanent snow and ice.

Depth increment	n:	Landscape mean SOC storage ($\text{kg C/m}^{2.2}$)	95 % CI ^a	Total SOC in Pg	95 % CI ^a
0–30 cm	452	9.0	± 1.4	160.0	± 25
30–50 cm	402	12.83.9	± 1.80.5	229.369.2	± 328
50–100 cm	328	21.38.4	± 3.21.4	379.7150.5	± 5825
100–200 cm	257	12.4	± 1.9	222.0	± 35
200–300 cm	253	11.8	± 1.7	211.0	± 31
0–100 cm	328	21.3	± 3.2	379.7	± 58
0–300 cm	253	45.5	± 7.6	812.6	± 136

352 ^a The 95 % confidence interval refers to landscape mean SOC storage and total SOC storage

354 Table 5: Mean and total SOC storage for (A) 0–100 cm and (B) 0–300 cm soil depth separated for the different Tier
 355 classes in the northern circumpolar permafrost region, excluding water bodies and permanent snow and ice.

A	Tier class	LCC class	n ^a :	Area (million km ²)	Area %	Mean SOC storage (kg C/m ²)	SD ^b	Total SOC in Pg	Total SOC storage %	
	1.1	Deciduous forest	broadleaf	5	0.85	4.8 %	16.5	9.3	14.1	3.7
	1.2	Evergreen forest	needleleaf	4	2.54	14.3 %	14.6	12.8	37.1	9.8
	1.3	Deciduous forest	needleleaf	28	5.20	29.1 %	20.5	20.3	106.5	28.1
	2.1	Shrub tundra		54	3.97	22.3 %	22.3	21.7	88.5	23.3
	2.2	Graminoid / forb tundra		118	2.85	15.9 %	31.6	23.0	90.0	23.7
	3.1	Permafrost wetlands		61	0.25	1.4 %	37.8	37.8	9.6	2.5
	3.2	Non-permafrost wetlands		10	0.76	4.3 %	17.8	14.7	13.5	3.6
	5.1	Barren		39	0.85	4.8 %	9.4	12.0	8.0	2.1
	7.1	Yedoma tundra		8	0.27	1.5 %	28.1	17.0	7.7	2.0
	7.2	Yedoma forest		1	0.30	1.7 %	16.1	0.0	4.8	1.3

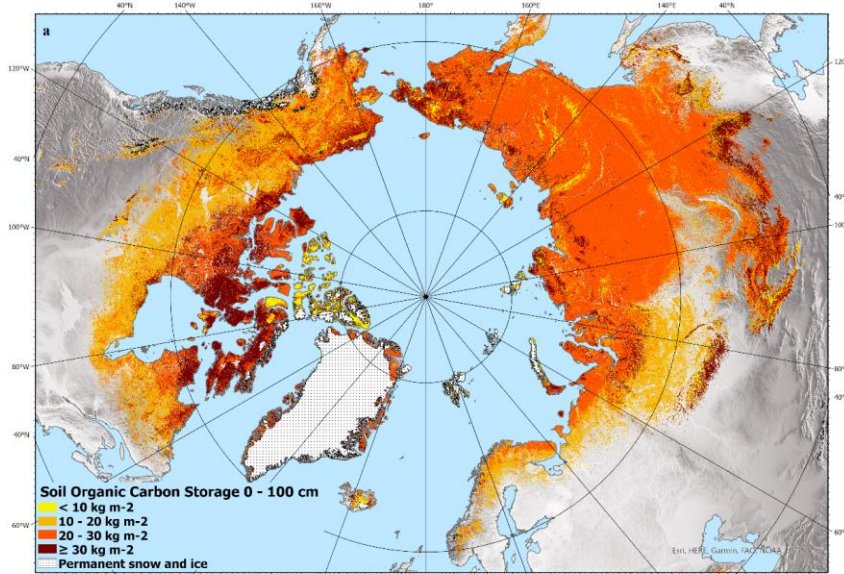
B	Tier class	LCC class	n ^a :	Area (million km ²)	Area %	Mean SOC storage (kg C/m ²)	SD ^b	Total SOC in Pg	Total SOC storage %	
	1.1	Deciduous forest	broadleaf	2	0.85	4.8 %	33.2	22.8	28.3	3.5
	1.2	Evergreen forest	needleleaf	2	2.54	14.3 %	23.0	16.3	58.7	7.2
	1.3	Deciduous forest	needleleaf	14	5.20	29.1 %	38.3	33.3	199.2	24.5
	2.1	Shrub tundra		50	3.97	22.3 %	49.2	50.8	195.6	24.1
	2.2	Graminoid / forb tundra		114	2.85	15.9 %	72.2	67.5	205.4	25.3
	3.1	Permafrost wetlands		49	0.25	1.4 %	112.2	121.5	28.4	3.5
	3.2	Non-permafrost wetlands		7	0.76	4.3 %	74.5	70.5	56.6	7.0
	5.1	Barren		9	0.85	4.8 %	11.7	14.9	10.0	1.2
	7.1	Yedoma tundra		5	0.27	1.5 %	64.1	37.7	17.5	2.2
	7.2	Yedoma forest		1	0.30	1.7 %	43.0	0.0	13.0	1.6

Formatted Table

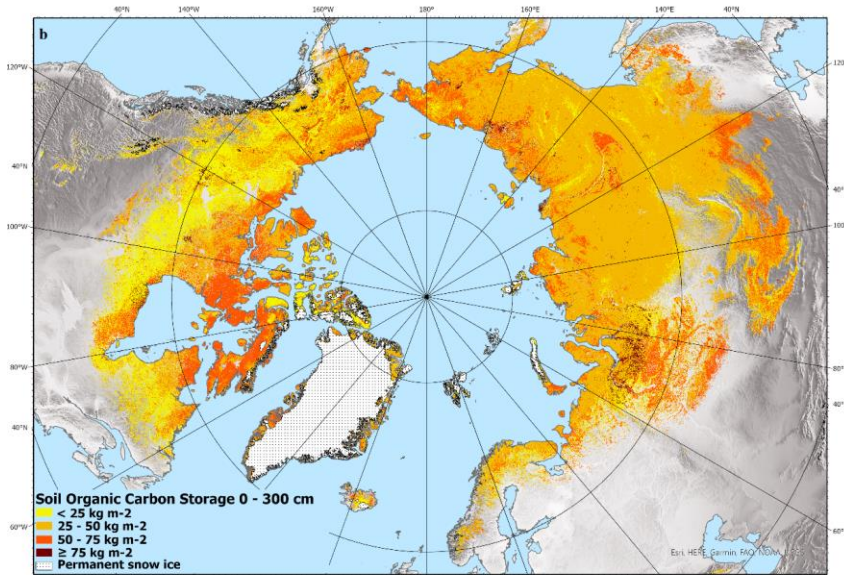
356

357 ^a The number of sampled pedons reaching a full depth of 100 cm or 300 cm, respectively.

358 ^b Mean SOC storage and SD calculations includes pedons which are not reaching the full section depth.



359



360

361 Estimated total SOC storage (kg C m⁻²) to a depth of 0–100 cm (a) and 0–300 cm (b) in northern circumpolar

Figure 3.

362 permafrost region. North Pole Lambert azimuthal equal area projection (datum: WGS 84). Base map: Made with
363 Natural Earth.

364 **3.2 TN estimates**

365 Our estimates show that the TN stocks down to 100 cm and 300 cm depth in the northern circumpolar permafrost
366 region are 21.1 Pg and 55.0 Pg, respectively. Table 6 presents the mean and total TN storage for different depth
367 increments with their 95% confidence interval. ~~The TN distribution throughout the full depth is more evenly~~
368 ~~distributed compared to SOC~~. As with SOC storage, the most abundant land cover classes (deciduous needleleaf forest,
369 shrub tundra and graminoid / forb tundra) store ~~the bulkmost~~ (68 %) of the total TN in the permafrost region. The land
370 cover classes permafrost and non-permafrost wetlands have the largest TN storage with a mean of up to 7 kg N m^{-2}
371 for the 0–300 cm soil depth (Table 7). Figure 4 illustrates the spatial distribution of total TN storage (kg N m^{-2}) for
372 the circumpolar permafrost region for two depth intervals, 0–100 cm and 0–300 cm. ~~The spatial distribution of TN~~
373 ~~has a similar pattern to SOC and is highlighting the permafrost peatlands in Western Siberia, Russia and the Nunavut~~
374 ~~territory in Canada.~~

375 Table 6: Mean and total TN storage with 95 % CI for the different depth increments for the northern circumpolar
376 permafrost region, excluding water bodies and permanent snow and ice.

Depth increment	Landscape mean TN storage (kg N m^{-2})	95 % CI ^a	Total TN in Pg	95 % CI ^a
0–30 cm	271	0.5	± 0.1	8.1 ± 1.5
30–50 cm	250	0.72	± 0.40	12.34.2 ± 02.5
50–100 cm	208	0.51.2	± 0.13	21.18.8 ± 4.71.1
100–200 cm	175	1.0	± 0.2	17.1 ± 2.8
200–300 cm	169	0.9	± 0.2	16.8 ± 3.7
0–100 cm	208	1.2	± 0.3	21.1 ± 4.7
0–300 cm	169	3.1	± 0.8	55.0 ± 15.1

377

378 ^a The 95 % confidence interval refers to landscape mean TN storage and total TN storage

379 Table 7: Mean and total TN storage for (A) 0–100 cm and (B) 0–300 cm soil depth separated for the different Tier
 380 classes within the northern circumpolar permafrost region, excluding water bodies and permanent snow and ice.

A	Tier class	LCC class	n ^a :	Area (million km ²)	Area %	Mean TN storage (kg N/m ²) ^b			Total TN in Pg	Total TN storage %
						SD ^b	Total	in		
1.1	Deciduous forest	broadleaf	2	0.85	4.8 %	1.0	0.6	0.9	4.1	
1.2	Evergreen forest	needleleaf	1	2.54	14.3 %	0.8	0.8	1.9	9.2	
1.3	Deciduous forest	needleleaf	19	5.20	29.1 %	1.0	0.6	5.1	24.3	
2.1	Shrub tundra		32	3.97	22.3 %	1.6	1.5	6.4	30.3	
2.2	Graminoid / forb tundra		72	2.85	15.9 %	1.5	0.9	4.3	20.3	
3.1	Permafrost wetlands		46	0.25	1.4 %	2.4	2.5	0.6	2.8	
3.2	Non-permafrost wetlands		4	0.76	4.3 %	0.7	0.6	0.5	2.4	
5.1	Barren		26	0.85	4.8 %	0.7	0.9	0.6	2.6	
7.1	Yedoma tundra		5	0.27	1.5 %	1.6	0.6	0.4	2.0	
7.2	Yedoma forest		1	0.30	1.7 %	1.4	0.0	0.4	2.0	

B	Tier class	LCC class	n ^a :	Area (million km ²)	Area %	Mean TN storage (kg N/m ²) ^b			Total TN in Pg	Total TN storage %
						SD ^b	Total	in		
1.1	Deciduous forest	broadleaf	2	0.85	4.8 %	2.8	1.7	2.4	4.3	
1.2	Evergreen forest	needleleaf	1	2.54	14.3 %	1.9	2.3	4.8	8.8	
1.3	Deciduous forest	needleleaf	12	5.20	29.1 %	2.4	1.3	12.6	23.0	
2.1	Shrub tundra		30	3.97	22.3 %	3.9	3.4	15.5	28.2	
2.2	Graminoid / forb tundra		69	2.85	15.9 %	3.4	2.2	9.6	17.5	
3.1	Permafrost wetlands		40	0.25	1.4 %	7.0	7.8	1.8	3.2	
3.2	Non-permafrost wetlands		2	0.76	4.3 %	6.4	6.6	4.9	8.9	
5.1	Barren		9	0.85	4.8 %	0.8	1.1	0.7	1.2	
7.1	Yedoma tundra		3	0.27	1.5 %	5.6	2.2	1.5	2.8	
7.2	Yedoma forest		1	0.30	1.7 %	4.1	0.0	1.2	2.2	

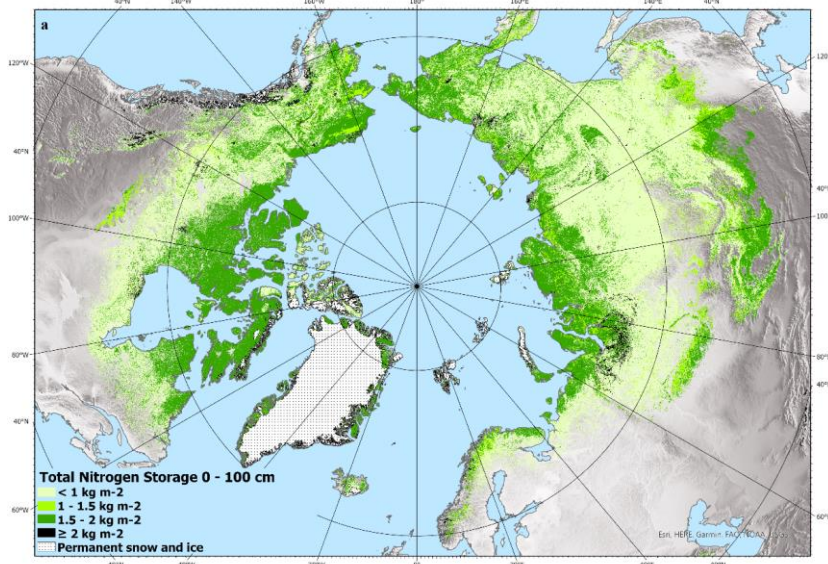
Formatted Table

381

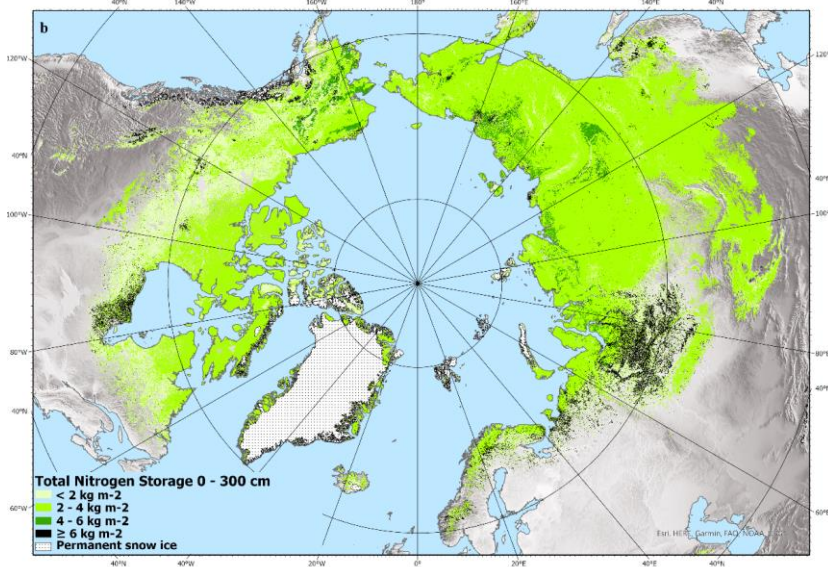
382 ^a The number of sampled pedons reaching a full depth of 100 cm or 300 cm, respectively.

383 ^b Mean TN storage and SD calculations includes pedons which are not reaching the full section depth.

384



385

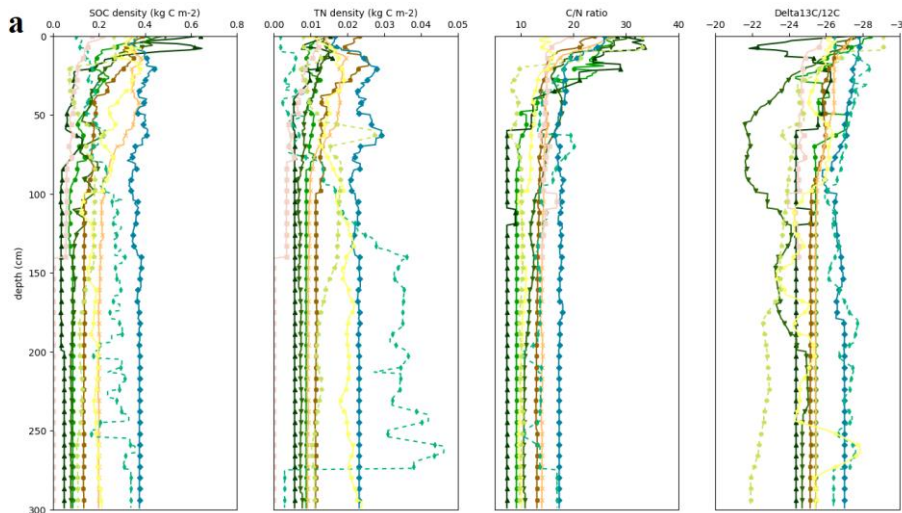


386

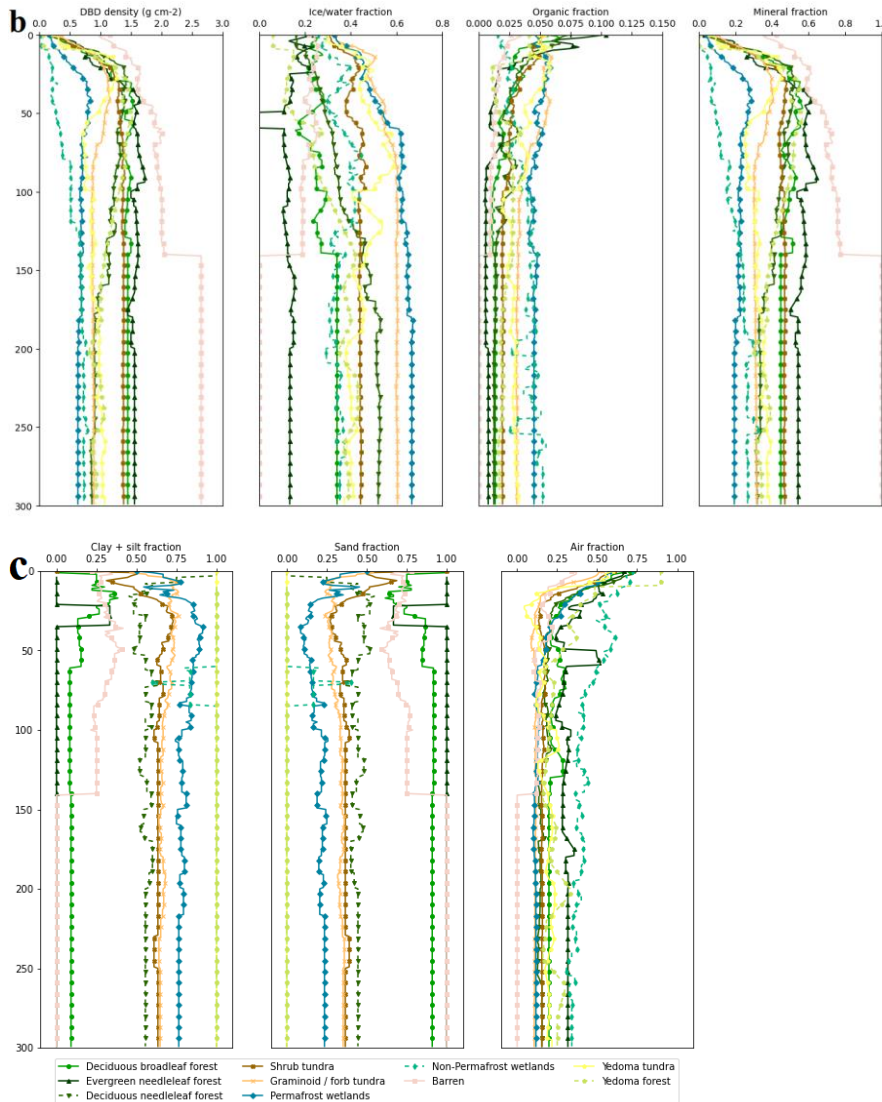
387 Figure 4. Estimated total Nitrogen storage (kg NC m⁻²) to a depth of 0–100 cm and 0–300 cm in northern circumpolar
 388 permafrost region. North Pole Lambert azimuthal equal area projection (datum: WGS 84). Base map: Made with
 389 Natural Earth.

390 **3.3 Typical vertical soil stratigraphies to 300 cm depth**

391 Figure 5 illustrates averaged vertical soil stratigraphies for SOC and TN density, C/N ratio with $\delta^{13}\text{C}_{\text{PDB}}$, dry bulk
392 density, volumetric fractions for water/ice, organic, mineral, air and texture (sand, silt+clay fraction) separated by
393 land cover class to 300 cm depth. The data shows clear differences occurring in the more variable top meter in
394 comparison to the rather stable second and third meter. With an exception in Non-Permafrost wetlands where the TN
395 and SOC density is more variable below 100 cm depth, which results from only 2 stratigraphy different available
396 pedons where TN data is available (Table 7). Instead, the Permafrost wetland class shows the highest and rather stable
397 stratigraphy for SOC and TN density, which is also supported by the high organic fraction with low DBD and low
398 mineral fraction. Which is the opposite for the Barren class with low SOC and TN surrounded by mainly coarse
399 mineral fraction and from ca. 140 cm depth where also our deepest barren samples reached bedrock. These important
400 trends are more evident, e.g. high variability in water fraction between classes or high silt+clay fraction, in Yedoma
401 tundra. We note that mineral soil texture is mainly determined by the parent material origin, which has not been
402 accounted for in the generation of these profiles.



405



406

407 Figure 5. Typical vertical soil stratigraphies for all the land cover classes to 300 cm depth [separated for SOC density,](#)
 408 [TN density, C/N ratio and Delta 13C/12C \(a\); DBD density, Ice/water fraction, Organic fraction and Mineral fraction](#)
 409 [\(b\); Clay + silt fraction, Sand fraction and Air fraction \(c\).](#)

410 **4. Discussion**

411 The goal of the field studies to collect this dataset has mainly been to improve the knowledge base for studies of
412 climate feedbacks resulting from permafrost thaw. This new open access database provides was created to serve
413 different scientific communities with high spatial resolution, harmonized and georeferenced data on soil organic
414 carbon and related key pedological parameters representative for large areas across the northern permafrost region.
415 Ggeoreferenced and quality assessed soil profile data to serve different scientific communities., with extensive
416 metadata will allow users to relate this field data to various other ecosystem properties or processes. The goal of the
417 field studies to collect this dataset has mainly been to improve the knowledge base for studies of climate feedbacks
418 resulting from permafrost thaw. While there are multiple databases available containing data on soil carbon storage
419 (Hugelius et al., 2013, Michaelson et al., 2013, Mishra et al., 2021), there is still a lack of soil field data covering a
420 wider range of properties within the hard-accessible northern circumpolar permafrost region. This database provides
421 detailed high resolution soil profile data on different key soil properties for both chemical (organic carbon, total
422 carbon, total nitrogen, d13C) and physical (dry and wet bulk density, soil texture, coarse fragments) parameters.

423 To test and exemplify usage of the soil profile database, we used our field-based metadata to classify soil profiles
424 according to a coherent land cover scheme and combined it with ESA's land cover product to provide a new estimate
425 of soil organic carbon storage in the northern circumpolar permafrost region. Our estimate for SOC is $380 \text{ Pg} \pm 58 \text{ Pg}$
426 to 100 cm soil depth and $813 \text{ Pg} \pm 136 \text{ Pg}$ to 300 cm soil depth for the permafrost region occupying an area of
427 $17.9 \times 10^6 \text{ km}^2$ (excluding area of Tibetan permafrost region, permanent snow and ice and water bodies). In
428 comparison, Hugelius et al., (2014) estimated SOC stocks in the northern circumpolar permafrost region (17.8×10^6
429 km^2 excluding exposed bedrock, glaciers and ice-sheets and water bodies) to be $472 \pm 27 \text{ Pg}$ and $1035 \pm 150 \text{ Pg}$ to
430 100 cm and 300 cm for soils, respectively. A recent publication by Mishra et al., (2021) based on >2700 soil profiles
431 with environmental variables in a geostatistical mapping framework, estimated a total SOC stock of 510 Pg (-78 to
432 $+79 \text{ Pg}$) and 1000 (-170 to $+186 \text{ Pg}$) to 100 cm and 300 cm, respectively. Although our values are a bit lower than
433 their estimates, they are within each other errors. Usage of a different landcover based upscaling approach could be
434 the cause of some of these differences. Despite different approaches in upscaling, with Hugelius et al., (2014) using
435 regional soil maps and Mishra et al., (2021) digital soil mapping, our landcover based estimate is on the lower edge
436 to previous studies. However, our estimates are still within each other's error estimates. In comparison, this upscaling
437 technique offers further benefits as this database can be easily extended with additional sampling sites, higher
438 resolution land cover maps that will further increase the resolution on a circumpolar scale. This data can also be used
439 for upscaling in a particular area of interest.

440 Despite the importance of nitrogen for microbial decomposition and plant productivity processes, few large-scale
441 datasets are available on TN storage. Our TN estimate for the northern circumpolar permafrost region is $21 \text{ Pg} \pm 5 \text{ Pg}$
442 to 100 cm soil depth and $55 \text{ Pg} \pm 15 \text{ Pg}$ to 300 cm soil depth. This is in line with the only other circumpolar estimate
443 of $66 \text{ Pg} (\pm 35 \text{ Pg})$ known to use by Harden et al. (2012) with a best estimate of $66 \text{ Pg} (\pm 35 \text{ Pg})$.

444 In addition, C/N ratio is a useful indicator of the organic matter decomposability which usually decreases with depth
445 with least decomposed material at the surface (organic layer) followed by carbon enriched (cryoturbated) pockets and
446 with smallest values and the most degraded material the mineral subsoil. Therefore, the C/N data together with the
447 ~~d13C~~ data locates the areas which are most likely to be more vulnerable to permafrost degradation which can be used
448 as a vulnerability map in combination with the botanical origin of the plant species using carbon isotopes.

449 A key element to this upscaling exercise is the accuracy of the land cover dataset. Despite the relatively high spatial
450 resolution of 300 m, many Arctic landscape features cannot be represented at this scale. ~~In addition~~Although, ESA's
451 land cover map has a good overall accuracy of 73 %; however, this means that 27 % of the land cover is possibly
452 mismatched and in need of improvement. Moreover, the accuracy for natural and semi-natural aquatic vegetation is
453 unfortunately as low as 19 % ~~which~~This corresponds to ~~the~~our class (wetland) ~~with the largest SOC content in the~~used in this
454 ~~permafrost region~~study. According to Hugelius et al. (2020), the areal extent of peatlands for the northern permafrost region
455 (3.7×10^6 km 2) is almost four times the ESA's land cover product estimated areal extent (1.0×10^6 km 2)~~, used in this~~study. ~~Therefore, wrongly classified areas~~This would partly explain our ~~throughout~~ lower estimate for SOC and TN
456 on a circumpolar scale since the wetland classes have the largest SOC and TN contents, particularly at greater depths
457 (100–300 cm). ~~Which is also visible on maps (Figure 3 and Figure 4) where areas classified as peatlands standing~~used in this
458 ~~out~~study. If we ~~exchange the ESA wetland areal coverage for the values from Hugelius et al. (2020)~~ correct the wetland area
459 to 3.7×10^6 km 2 (2.0×10^6 km 2 in permafrost-free peatlands and 1.7×10^6 km 2 permafrost-affected peatlands) and
460 deduct this in proportion from the other classes, our updated SOC and TN stock to 300 cm soil depth increases ~~from~~used in this
461 $813 \text{ Pg} \pm 136 \text{ Pg}$ to $954 \text{ Pg} \pm 162 \text{ Pg}$ and ~~from~~used in this $55 \text{ Pg} \pm 15 \text{ Pg}$ to $66 \text{ Pg} \pm 22 \text{ Pg}$, respectively.

462
463 Even though the current estimates are based on 651 soil pedons from 16 different study areas, there are uncertainties
464 and data gaps for several regions and ecosystems. With e.g. only one high alpine site and one Yedoma forest site,
465 several areas are highly underrepresented. Also, the study areas are concentrated in European and Russian locations
466 which additionally increases the uncertainties in current estimates. Therefore, combining this data with other datasets
467 especially from North America, Tibet, Yedoma sites and a different wetland extent would substantially reduce
468 potential error sources and create a more complete picture of SOC and TN storage estimates from land cover based
469 upscaling.

470 To our knowledge, this is the first product which presents ~~a more complete dataset in regard to variables different key~~
471 ~~soil properties and parameters~~ on a circumpolar scale ~~even though they are the ones~~ that are commonly used to
472 parameterize earth system models. With this database we aim to provide georeferenced point data that can easily be
473 implemented and used for geospatial analysis at a circumpolar scale. This upscaling approach was chosen because
474 this database can be easily extended with additional sampling sites, higher-resolution land cover maps that will further
475 increase the resolution on a circumpolar scale. This data can also be used for upscaling in a particular area of interest.
476 This will assist to quantify and model ongoing pedological and ecological processes relevant to climate change.
477 Furthermore, this may help identifying regions that are more vulnerable to permafrost degradation and greenhouse
478 gas release due to knowledge on texture, water/ice content or SOC storage.

479 **5. Conclusion**

480 This dataset represents a substantial contribution of high-quality soil pedon data and metadata across the northern
481 permafrost region. Despite a different methodology, our land cover based estimates of total SOC to 100 cm and 300
482 cm soil depth are 380 Pg ± 58 Pg and 813 Pg ± 136 Pg, respectively. In addition to SOC data, we contribute with
483 novel TN estimates for the different land cover classes and depth increments. Our TN estimate to 100 cm and 300 cm
484 soil depth are 21.1 ± 4.7 Pg and (55 Pg ± 15 Pg) which is in line with the only other product available on that scale
485 for TN. Despite a different methodology, are similar but on the lower edge to other recent numbers, are similar but on
486 the lower edge to other recent numbers. The lower estimates from our dataset are probably due to underestimated areal
487 extent of northern peatlands in the ESA Global Land Cover dataset. In addition to SOC data, we contribute with novel
488 TN estimates for the different land cover classes and depth increments. Our TN estimate to 300 cm soil depth (55 Pg
489 ± 15 Pg) is in line with the only other product available on that scale. We provide data for a wide range of environments
490 and geographical regions across the permafrost region including georeferencing and metadata. This serves as a base
491 that can be easily combined and extended with data from other sources, as several regions are underrepresented
492 (Alaska, Canada, Tibet). This dataset offers high scientific value as it also contains data on chemical and physical soil
493 properties across the northern circumpolar permafrost region. This additional data is of high importance and can be
494 used to develop or parametrize broad scale models and to help better understand different aspects of the permafrost-
495 carbon climate feedback.

496 **6. Data access**

497 Two separated datasets are freely available on the Bolin Centre data set repository (<https://bolin.su.se/data/>). The
498 dataset (Detailed pedon data on soil carbon and nitrogen for the northern permafrost region,
499 <https://doi.org/10.17043/palmtag-2022-pedon-1>) (Palmtag et al., 2022a) is a geospatial dataset of physical and
500 chemical soil properties from 651 soil pedons and the second dataset (A high spatial resolution soil carbon and nitrogen
501 dataset for the northern permafrost region, <https://doi.org/10.17043/palmtag-2022-spatial-1>) (Palmtag et al., 2022b)
502 contains GIS grids of the northern circumpolar permafrost region for SOC, TN and C/N ratios for the different depth
503 increments, with GeoTiffs (Palmtag et al., 2022b) are freely available on the Bolin Centre data set repository ().

504 Field Code Changed

505 **Funding**

506 This study was funded through the European Space Agency CCI + Permafrost project (4000123681/18/I-NB), the
507 European Union Horizon 2020 research and innovation project Nunataryuk (773421), the Changing Arctic Ocean
508 (CAO) program project CACOON (NE/R012806/1) and the Swedish Research Council (2018-04516).

509

510 **Author contribution**

511 GH, PK, SW and JP designed the concept of the study. JO wrote the script in Python. JP wrote the initial draft of the
512 manuscript. All authors contributed to the writing and editing of the manuscript.

513 **Competing Interests**

514 The authors declare that they have no conflict of interest.

515 **Acknowledgements**

516 We thank the ESA CCI Land Cover project for providing the data, which was used for upscaling our product to
517 circumpolar scale.

518 **References**

519 Batjes, N.H.: Harmonized soil property values for broad-scale modelling (WISE30sec) with estimates of global soil
520 carbon stocks, *Geoderma*, Vol. 269, <https://doi.org/doi.org/10.1016/j.geoderma.2016.01.034>, 2016.

521 Biskaborn, B. K., Smith, S. L., Noetzli, J., Matthes, H., Vieira, G., Streletschi, D. A., Schoeneich, P., Romanovsky,
522 V. E., Lewkowicz, A. G., Abramov, A., Allard, M., Boike, J., Cable, W. L., Christiansen, H. H., Delaloye, R.,
523 Diekmann, B., Drozdov, D., Etzelmüller, B., Grosse, G., Guglielmin, M., Thomas Ingeman-Nielsen, T., Ketil Isaksen,
524 K., Ishikawa, M., Johansson, M., Johannsson, H., Joo, A., Kaverin, D., Kholodov, A., Konstantinov, P., Kröger, T.,
525 Lambiel, C., Lanckman, J.-P., Luo, D., Malkova, G., Meiklejohn, I., Moskalenko, N., Oliva, M., Phillips, M., Ramos,
526 M., Sannel, A. B. K., Sergeev, D., Seybold, C., Skryabin, P., Vasiliev, A., Wu, Q., Yoshikawa, K., Zheleznyak, M.
527 and Lantuit, H.: Permafrost is warming at a global scale, *Nature Communications*, 10(1), 264,
528 <https://doi.org/10.1038/s41467-018-08240-4>, 2019.

529 Czekirda, J., Westermann, S., Etzelmüller, B. and Johannesson, T.: Transient modelling of permafrost distribution in
530 Iceland. *Frontiers in Earth Science*, 7, 130, <https://doi.org/doi.org/10.3389/feart.2019.00130>, 2019.

531 Defourny, P., Schouten, L., Bartalev, S.A., Bontemps, S., Caccetta, P., de Wit, A.J.W., Di Bella, C., Gerard, B., Giri,
532 C., Gong, V., Hazeu, G.W., Heinemann, A., Herold, M., Knoops, J., Jaffrain, G., Latifovic, R., Lin, H., Mayaux, P.,
533 Mächer, C.A., Nonguierma, A., Stibig, H.J., Van Bogaert, E., Vancutsem, C., Bicheron, P., Leroy, M. and Arino, O.:
534 Accuracy assessment of a 300 m global land cover map: The GlobCover experience. Available online: <http://www.un-spider.org/space-application/space-application-matrix/accuracy-assessment-300-m-global-land-cover-map-globcover> (accessed on 07 January 2022), 2008.

537 ESA Climate Change Initiative-Landcover visualization interface, Available from:
538 <http://maps.elie.ucl.ac.be/CCI/viewer/index.php> (accessed on 07 January 2022), 2017.

539 Farouki, O. T.: Thermal Properties of Soils, Cold regions research and engineering lab Hanover NH [online] Available
540 from: <https://apps.dtic.mil/docs/citations/ADA111734> (accessed on 07 January 2022), 1981.

541 Flato, G. M.: Earth system models: an overview, 2, 783–800, <https://doi.org/10.1002/wcc.148>, 2011.

542 Fritz, M., Vonk, J.E. and Lantuit, H.: Collapsing Arctic coastlines, *Nature Climate Change*, volume 7,
543 <https://doi.org/10.1038/nclimate3188>, 2017.

544 Fuchs, M., Kuhry, P., and Hugelius, G.: Low below-ground organic carbon storage in a subarctic Alpine permafrost
545 environment, *The Cryosphere*, 9, 427–438, <https://doi.org/10.5194/tc-9-427-2015>, 2015.

546 Global Soil Data Task: Global soil data products CD-ROM contents (IGBP-DIS), ORNL DAAC, 2014.

547 Gruber, S.: Derivation and analysis of a high-resolution estimate of global permafrost zonation, *The Cryosphere*, 6,
548 221–233, <https://doi.org/10.5194/tc-6-221-2012>, 2012.

549 Harden, J.W., Koven, C.D., Ping, C.-L., Hugelius, G., McGuire, A.D., Camill, P., Jorgenson, T., Kuhry, P.,
550 Michaelson, G.J., O'Donnell, J.A., Schuur, E.A.G., Tarnocai, C., Johnson, K. and Grosse, G.: Field information links
551 permafrost carbon to physical vulnerabilities of thawing. *Geophysical Research Letter*, 39, L15704,
552 <https://doi.org/doi:10.1029/2012GL051958>, 2012.

553 Heiri, O., Lotter, A. F., and Lemcke, G.: Loss on ignition as a method for estimating organic carbon and carbonate
554 content in sediments: reproduction and comparability of results. *J. Paleolimnol.*, 25, 101–110,
555 <https://doi.org/10.1023/a:1008119611481>, 2001.

556 Hugelius G. and Kuhry, P.: Landscape partitioning and environmental gradient analyses of soil organic carbon in a
557 permafrost environment. *Global Biogeochem. Cycles*, 23, GB3006, <https://doi.org/doi:10.1029/2008GB003419>,
558 2009.

559 Hugelius G., Kuhry, P., Tarnocai, C. and Virtanen, T.: Soil organic carbon pools in a periglacial landscape: a case
560 study from the central Canadian Arctic. *Permafrost Periglac. Process.*, 21: 16–29. <https://doi.org/10.1002/ppp.677>,
561 2010.

562 Hugelius, G., Virtanen, T., Kaverin, D., Pastukhov, A., Rivkin, F., Marchenko, S., Romanovsky, V. and Kuhry, P.:
563 High-resolution mapping of ecosystem carbon storage and potential effects of permafrost thaw in periglacial terrain,
564 European Russian Arctic, *J. Geophys. Res.*, 116, G03024, <https://doi.org/doi:10.1029/2010JG001606>, 2011.

565 Hugelius, G., 2012.: Spatial upscaling using thematic maps: An analysis of uncertainties in permafrost soil carbon
566 estimates. *Global Biogeochem Cycles* GB2026. <https://doi.org/doi:10.1029/2011GB004154, 2012>.

567 Hugelius, G., Bockheim, J. G., Camill, P., Elberling, B., Grosse, G., Harden, J. W., Johnson, K., Jorgenson, T., Koven,
568 C. D., Kuhry, P., Michaelson, G., Mishra, U., Palmtag, J., Ping, C.-L., O'Donnell, J., Schirrmeyer, L., Schuur, E. A.
569 G., Sheng, Y., Smith, L. C., Strauss, J., and Yu, Z: A new data set for estimating organic carbon storage to 3 m depth
570 in soils of the northern circumpolar permafrost region. *Earth Syst. Sci. Data*, 5, 393–402, <https://doi.org/10.5194/essd-5-393-2013>, 2013.

572 Hugelius, G., Strauss, J., Zubrzycki, S., Harden, J. W., Schuur, E. A. G., Ping, C.-L., Schirrmeister, L., Grosse, G.,
573 Michaelson, G. J., Koven, C. D., O'Donnell, J. A., Elberling, B., Mishra, U., Camill, P., Yu, Z., Palmtag, J., and Kuhry,
574 P.: Estimated stocks of circumpolar permafrost carbon with quantified uncertainty ranges and identified data gaps.
575 *Biogeosciences* 11(23):6573– 6593, <https://doi.org/10.5194/bg-11-6573-2014>, 2014.

576 Hugelius, G., Loisel, J., Chadburn, S., Jackson, R.B., Jones, M., MacDonald, G., Marushchak, M., Olefeldt, D.,
577 Packalen, M., Siewert, M.B., Treat, C., Turetsky, M., Voigt, C. and Yu, Z.: Large stocks of peatland carbon and
578 nitrogen are vulnerable to permafrost thaw. *PNAS*, 117, 34,
579 <https://doi.org/www.pnas.org/cgi/doi/10.1073/pnas.1916387117>, 2020.

580 Köchy, M., Hiederer, R., and Freibauer, A.: Global distribution of soil organic carbon – Part 1: Masses and frequency
581 distributions of SOC stocks for the tropics, permafrost regions, wetlands, and the world, *SOIL*, 1, 351–365,
582 <https://doi.org/10.5194/soil-1-351-2015>, 2015.

583 Kracht, O and Gleixner, G.: Isotope analysis of pyrolysis products from Sphagnum peat and dissolved organic matter
584 from bog water. *Organic Geochemistry* , 31: 645–654, [https://doi.org/10.1016/S0146-6380\(00\)00041-3](https://doi.org/10.1016/S0146-6380(00)00041-3), 2020.

585 Kuhry, P. and Vitt, D.H.: Fossil Carbon/Nitrogen Ratios as a Measure of Peat Decomposition. *Ecology*, 77: 271-275.
586 <https://doi.org/10.2307/2265676>, 1996.

587 Kuhry, P., Mazhitova, G.G., Forest, P.-A., Deneva, S.V., Virtanen, T. and Kultti, S.: Upscaling soil organic carbon
588 estimates for the Usa Basin (Northeast European Russia) using GIS-based land cover and soil classification schemes.
589 *Geografisk Tidsskrift-Danish Journal of Geography*, 102:1, 11-25, <https://doi.org/10.1080/00167223.2002.10649462>, 2002.

591 McKinney, W.: "pandas: a foundational Python library for data analysis and statistics." Python for high performance
592 and scientific computing 14.9, 1-9, 2011.

593 Michaelson, G.J., Ping, C.-L. and Clark, M.: Soil Pedon Carbon and Nitrogen Data for Alaska: An Analysis and
594 Update. *Open Journal of Soil Science*, 2013, 3, 132-142 <http://dx.doi.org/10.4236/ojss.2013.32015>, 2013.

595 Mishra, U., Hugelius, G., Shelef, E., Yang, Y., Strauss, J., Lupachev, A., Harden, J.W., Jastrow, J.D., Ping, C.-L.,
596 Riley, W.J., Schuur, E.A.G., Matamala, R., Siewert, M., Nave, L.E., Koven, C.D., Fuchs, M., Palmtag, J., Kuhry, P.,
597 Treat, C.C., Zubrzycki, S., Hoffman, F.M., Elberling, B., Camill, P., Veremeeva, A. and Orr, A.: Spatial heterogeneity
598 and environmental predictors of permafrost region soil organic carbon stocks. *Science Advances*, 7, 9,
599 <https://doi.org/10.1126/sciadv.aaz5236>, 2021.

600 Nachtergaele, F., van Velthuizen, H., Verelst, L., Batjes, N.H., Dijkshoorn, K., van Engelen, V.W.P., Fischer, G.,
601 Jones, A. and Montanarella, L.: The harmonized world soil database, in Proceedings of the 19th World Congress of
602 Soil Science, Soil Solutions for a Changing World, Brisbane, Australia, 1-6 August 2010, pp. 34–37, 2010.

603 National Wetlands Working Group. The Canadian Wetland Classification System, 2nd Edition. Warner, B.G. and
604 C.D.A. Rubec (eds.), Wetlands Research Centre, University of Waterloo, Waterloo, ON, Canada. 68 p, 1997.

Field Code Changed

Formatted: No underline

605 Obu, J., Westermann, S., Bartsch, A., Berdnikov, N., Christiansen, H.H., Dashtseren, A., Delaloye, R., Elberling, B.,
606 Etzelmuller, B., Kholodov, A., Khomutov, A., Kääb, A., Leibman, M.O., Lewkowicz, A.G., Panda, S.K.,
607 Romanovsky, V., Way, R.G., Westergaard-Nielsen, A., Wu, T., Yamkhin, J. and Zou, D.: Northern Hemisphere
608 permafrost map based on TTOP modelling for 2000–2016 at 1 km² scale, *Earth-Science Reviews* 193,
609 <https://doi.org/10.1016/j.earscirev.2019.04.023>, 2019.

610 Obu, J.: How much of the Earth's surface is underlain by permafrost? *Journal of Geophysical Research: Earth Surface*,
611 126, e2021JF006123. <https://doi.org/10.1029/2021JF006123>, 2021

612 Oleson, K. W., Lawrence, D. M., Bonan, G.B., Flanner, M.G., Kluzek, E., Lawrence, P.J., Levis, S., Swenson, S.C.,
613 Thornton, P.E., Dai, A., Decker, M., Dickinson, R., Feddema, J., Heald, C.L., Hoffman, F., Lamarque, J.-F.,
614 Mahowald, N., Niu, G.-Y., Qian, T., Randerson, J., Running, S., Sakaguchi, K., Slater, A., Stockli, R., Wang, A.,
615 Yang, Z.-L., Zeng, X., and Zeng, X.: Technical description of version 4.0 of the Community Land Model (CLM),
616 2010.

617 Palmtag, J., Hugelius, G., Lashchinskiy, N., Tarmstorf, M.P., Richter, A., Elberling, B. and Kuhry, P.: Storage,
618 landscape distribution and burial history of soil organic matter in contrasting areas of continuous permafrost, *Arct. Antarct. Alp. Res.*, 47, 71–88, <https://doi.org/10.1657/AAAR0014-027>, 2015.

620 Palmtag, J., Ramage, J., Hugelius, G., Gentsch, N., Lashchinskiy, N., Richter, A. and Kuhry, P.: Controls on the
621 storage of organic carbon in permafrost soils in northern Siberia, *Eur. J. Soil Sci.*, 67, 478–491,
622 <https://doi.org/10.1111/ejss.12357>, 2016.

623 Palmtag, J. and Kuhry, P.: Grain size controls on cryoturbation and soil organic carbon density in permafrost-affected
624 soils. *Permafrost and Periglac Process*, 29, <https://doi.org/10.1002/ppp.1975>, 2018.

625 Palmtag, J., Obu, J., Kuhry, P., Siewert, M., Weiss, N. and Hugelius, G.: Detailed pedon data on soil carbon and
626 nitrogen for the northern permafrost region. Dataset version 1. Bolin Centre Database.
627 <https://doi.org/10.17043/palmtag-2022-pedon-1>, 2022a.

628 Palmtag, J., Obu, J., Kuhry, P., Siewert, M., Weiss, N. and Hugelius, G.: A high spatial resolution soil carbon and
629 nitrogen dataset for the northern permafrost region. Dataset version 1. Bolin Centre Database.
630 <https://doi.org/10.17043/palmtag-2022-spatial-1>, 2022b.

631 Pascual, D., Kuhry, P. and Raudina, T.: Soil organic carbon storage in a mountain permafrost area of Central Asia
632 (High Altai, Russia). *Ambio*. <https://doi.org/10.1007/s13280-020-01433-6>, 2020.

633 Pribyl, D. W.: A critical review of the conventional SOC to SOM conversion factor, *Geoderma*, 156(3), 75–83,
634 <https://doi.org/doi:10.1016/j.geoderma.2010.02.003>, 2010.

635 Siewert, M.B., Hanisch, J., Weiss, N., Kuhry, P., Maximov, T.C. and Hugelius, G.: Comparing carbon storage of
636 Siberian tundra and taiga permafrost ecosystems at very high spatial resolution. *JGR - Biogeosciences*, Volume 120,
637 <https://doi.org/10.1002/2015JG002999>, 2015.

638 Siewert, M.B., Hugelius, G., Heim, B. and Faucherre, S.: Landscape controls and vertical variability of soil organic
639 carbon storage in permafrost-affected soils of the Lena River Delta. *CATENA*, Volume 147, Pages 725-741,
640 <https://doi.org/10.1016/j.catena.2016.07.048>, 2016.

641 Siewert, M. B.: High-resolution digital mapping of soil organic carbon in permafrost terrain using machine learning:
642 a case study in a sub-Arctic peatland environment, *Biogeosciences*, 15, 1663–1682, <https://doi.org/10.5194/bg-15-1663-2018>, 2018.

644 Siewert, M.B., Lantuit, H., Richter, A. and Hugelius, G.: Permafrost Causes Unique Fine-Scale Spatial Variability
645 Across Tundra Soils. *Global Biogeochemical Cycles*, 35, e2020GB006659. <https://doi.org/10.1029/2020GB006659>,
646 2021.

647 [Soil survey staff, 2014. Keys to Soil Taxonomy](#). Soil survey staff, 2014. *Keys to Soil Taxonomy*. United States Department of
648 Agriculture & Natural Resources Conservation Service, Washington, DC, 12th ed. edition. [Soil Taxonomy](#). United States
649 Department of Agriculture & Natural Resources Conservation Service, Washington, DC, 12th ed. edition.

650 Strauss, J., Schirrmeister, L., Grosse, G., Fortier, D., Hugelius, G., Knoblauch, C., Romanovsky, V., Schädel, C.,
651 Schneider von Deimling, T., Schuur, T.A.G., Shmelyov, D., Ulrich, M. and Veremeeva, A.: Deep Yedoma permafrost:
652 A synthesis of depositional characteristics and carbon vulnerability, *Earth-Science Reviews*, Volume 172,
653 <https://doi.org/10.1016/j.earscirev.2017.07.007>, 2017.

654 Thomson, S.K. Sampling. New York: John Wiley, 343 pp., 1992.

655 Turetsky, M.R., Abbott, B.W., Jones, M.C., Anthony, K.W., Olefeldt, D., Schuur, T.A.G., Koven, C., McGuire, A.D.,
656 Grosse, G., Kuhry, P., Hugelius, G., Lawrence, D.M., Gibson, C. and Sannel, A.B.K.: Permafrost collapse is
657 accelerating carbon release, *Nature*, 569, <https://doi.org/10.1038/d41586-019-01313-4>, 2019.

658 Weiss, N., Blok, D., Elberling, B., Hugelius, G., Jørgensen, C.J., Siewert, M.B. and Kuhry, P.: Thermokarst dynamics
659 and soil organic matter characteristics controlling initial carbon release from permafrost soils in the Siberian Yedoma
660 region. *Sedimentary Geology*, 340, 38-48, <https://doi.org/10.1016/j.sedgeo.2015.12.004>, 2016.

661 Weiss, N., Faucherre, S., Lampiris, N. and Wojcik, R.: Elevation-based upscaling of organic carbon stocks in High-
662 Arctic permafrost terrain: a storage and distribution assessment for Spitsbergen, Svalbard. *Polar Research*, 36,
663 <https://doi.org/10.1080/17518369.2017.1400363>, 2017.

664 Westermann, S., Schuler, T. V., Gisnås, K. and Etzelmüller, B.: Transient thermal modeling of permafrost conditions
665 in Southern Norway, *The Cryosphere*, 7, 719–739, <https://doi.org/10.5194/tc-7-719-2013>, 2013.

666 Westermann, S., Peter, M., Langer, M., Schwamborn, G., Schirrmeister, L., Etzelmüller, B., and Boike, J.: Transient
667 modeling of the ground thermal conditions using satellite data in the Lena River delta, Siberia, *The Cryosphere*, 11,
668 1441–1463, doi.org/10.5194/tc-11-1441-2017, 2017.

669 Wojcik, R., Palmtag, J., Hugelius, G., Weiss, N. and Kuhry, P.: Landcover and landform-based upscaling of soil
670 organic carbon stocks on the Brøgger Peninsula, Svalbard, *Arctic, Antarctic, and Alpine Research*, 51:1, 40-57,
671 <https://doi.org/DOI>: 10.1080/15230430.2019.1570784, 2019.